Nonlinear Dyn
https://doi.org/10.1007/s11071-021-06704-9

ORIGINAL PAPER

Diversity of neuronal activity is provided by hybrid synapses

Kesheng Xu · **Jean Paul Maidana** · **Patricio Orio**

Received: 21 March 2021 / Accepted: 3 July 2021

Abstract The coexistence of electrical and chemical synaptic communication among excitatory cells has been evidenced by neuroscientists. Nevertheless, theoretical understanding of hybrid synaptic connections in diverse dynamical states of neural networks for self-organization and robustness, still has not been fully studied. Here, we present a model of neural network that includes chemical excitatory coupling in a way of small-world topology and electrical synaptic coupling among adjacent excitatory cells for excitatory population. Firstly, we use this model to investigate the effect of electrical synaptic coupling among excitatory cells on global network behavior with the goal of theoretically understanding mechanisms of generating rich firing patterns. Secondly, we further study the emergence of various firing ripple events by considering the variation of chemical synaptic inhibition and other factors, such as network densities. We found that the excitatory population has a tendency to synchronization as the weights of electrical synaptic coupling among excitatory cells are increased. Moreover, the existence of these electrical synaptic connections can cause various firing patterns of interest by slightly changing the chemical synaptic weights. Our results pave a way in the study of the dynamical mechanisms and computational significance of the contribution of mixed synapse in the neural functions.

Keywords Hybrid synapses · Excitatory-inhibitory networks · Firing pattern

1 Introduction

Over the past decades, a variety of spatiotemporal patterns have been observed in experimental recordings of neural activity, such as synchronous states [1,2], complex spatiotemporal patterns [3–9] and chimera states [10,11]. They have long been of interest, but there still much to be known about their underlying mechanisms.

Neurons can communicate mainly by two modalities of synaptic transmission—chemical synapse (CS) and electrical synapse (ES) [12,13]. At chemical synapses, information is transferred through the release of a neurotransmitter from presynaptic neuron and detection of the neurotransmitter by an adjacent postsynaptic cell [14], whereas in electrical synapses, the cytoplasm of adjacent cells is directly connected by clusters of intercellular channels called gap junctions [15]. From this different characteristics and functionality, chemical synaptic communication is typically unidirectional

K. Xu (✉)
School of physics and Electronic Engineering, Jiangsu University, Zhenjiang 212013, Jiangsu, People's Republic of China
e-mail: ksxu@ujs.edu.cn

K. Xu · J. P. Maidana · P. Orio
Centro Interdisciplinario de Neurociencia de Valparaíso, Universidad de Valparaíso, 2360102 Valparaíso, Chile

P. Orio
Facultad de Ciencias, Instituto de Neurociencia, Universidad de Valparaíso, 2360102 Valparaíso, Chile

Published online: 02 August 2021

and episodic. By contrast, electrical synaptic transmission through gap junctions underlies direct, continuous, and rapid neuronal communication in the central nervous system (CNS) [15]. In addition, electrical synapses are mostly bidirectional and connect neurons that are spatially very close.

Classically, research efforts to understand the emergence and diversity of firing patterns have been put in networks connected by chemical synapses. This type of neuronal communication can be of either excitatory or inhibitory nature; and while excitatory neurons can only excite each other, inhibitory neurons can generate nonlinear effects [16], such as modulating stimulus response gain, sharpening tuning to stimuli, and pacing cortical oscillations [16,17]. The balance between coactivated excitatory and inhibitory synaptic inputs is largely recognized to be important for cortical circuits and their function [18–21] (for a review see ref. [17]). For example, when externally driven, circuits of recurrently connected by excitatory and inhibitory neurons settle rapidly into a stable dynamical state [22–24].

Electrical synapses were first evidenced in crayfish and the vertebrate CNS of teleost fish soon after (see review [25]). The first strong evidence for mammalian electrical synapse is in the inferior olivary nucleus [25]. Electrical synapses are now known to be presented throughout various brain regions, including neocortex, hippocampus, thalamic reticular nucleus, retina, and spinal cord [12,25–27]. Excitatory synapses are mainly located on dendritic spines [28], whereas inhibitory synapses are located on or near the soma of pyramidal cells as well as on dendritic shafts [29]. Recently, many experiments have evidenced that diverse neural circuits use a combination of electrical and chemical synapses—hybrid synapses—coexisting in most organisms and brain structures [30–33], to convey signals between neurons (reviewed in [12,27]). The corresponding biophysical effects of hybrid synapses together with their circuits on neuronal dynamics have been reviewed briefly (see figure 3 in [34]). Electrical coupling is responsible for a variety of network effects, particularly in networks that generate rhythmic activity, some of which are well established, such as regulation of phase relationships, synchrony, and pattern formation [35–39], and some are novel, such as a direct role in rhythmogenesis (also see review [2]).

A wealth of evidence indicates that electrical synapses are localized primarily in inhibitory neurons [25,40], widely distributed throughout the CNS [27,40–42]. Computer simulations have greatly contributed to reveal the impact and functional role of gap junctions between inhibitory interneurons on network activity. One of the most distinct and recognizable effects of the electrical synapses is to enhance synchronized neuronal firing [25,43]. Also, the presence of electrical synapses could mediate close synchronization of subthreshold and spiking activity among clusters of neurons [13,44]. In all, the role of electrical synapses for network activity has been the topic of various review articles (see Ref [40,45]).

More recent reports have provided evidence for abundant electrical synapses interlinking excitatory neurons. The best examples of electrical synapses occur between excitatory glutamatergic inferior olivary cells [46], glutamatergic excitatory trigeminal mesencephalic primary afferent neurons [47], excitatory glutamatergic retinal ganglion cells [48,49], and others (reviewed in [27]). However, the role of gap junction interlinking excitatory population in diversity of neural activity generation has not been investigated deeply in networks of varying complexities yet.

The relationship between spatiotemporal patterns of neuronal activity and the types of synaptic transmission can be investigated in modeling studies [50–53]. Computational models have shown that the synchronous occurrence of action potentials in many neurons is mainly due to connections of chemical inhibitory synapses [54–58] or electrical synapses between neurons [1,2,59–62]. Synchronous oscillations often comes from the interplay of chemical synapses between excitatory cells (E-cells) and inhibitory cells (I-cells) [54–58,63,64]. In addition, emergence of synchronization has also been well investigated in temporal or time-varing multiplex hypernetworks composed of Hindmarsh-Rose neurons connected by electrical synapses, chemical synapses, or both [65–68]. Synchronous states have traditionally been thought to involve precise zero-lag synchrony [69,70]. In addition to synchronous states, there exists a range of flexible phase offsets—phase differences between two (or more) oscillations. These flexible phase relationships can, in their simplest form, be traveling waves of various shapes waves [71]. The combination of multiple traveling waves can form complex spatiotemporal patterns [4,72]. It has been shown, in spiking neural networks [71,73–75]that transmission delays [61], the spatial reach of connections [7] and the strength of inhibition of the excitatory-inhibitory net-

works influence the emergence of spatiotemporal patterns, such as asynchronous and irregular activity, or propagating waves. Recently, much attention has been paid to the chimera state [76–82]. In chimera state, populations of coupled oscillators may exhibit two coexisting subpopulations, one with synchronized oscillations and the other with unsynchronized oscillations, even though all of the oscillators are coupled to each other in an equivalent manner [83,84]. This symmetry-breaking behavior has been studied in a variety of complex dynamical systems and has attracted growing attention in neural system studies from both theoretical and experimental perspectives [85–87].

All these approaches mentioned above only identify the essential mechanisms for generating various complex spatiotemporal patterns, such as synchrony state, chimeras state, and others, in neural networks coupled via electrical synapse, chemical synapse or combination of them—hybrid synapses. Nevertheless, they give little insight on how the electrical and chemical synapses are related to the emergence of a diversity of dynamical states in neural networks for self-organization and robustness. In other words, the contribution of electrical coupling between excitatory neurons together with their synaptic weights on neuronal spatiotemporal patterns has not been systematically investigated yet. For example, whether gap junction communicating the excitatory or inhibitory neurons make significant different contributions to generate firing patterns , and moreover whether these different states can coexist in the same parameter space or the same time windows of interest still have not been fully studied yet.

In this paper, we study the emergence of several firing patterns in an excitatory-inhibitory (E/I) balanced network, combining the effect of electrical and chemical connections. First, we report the several firing patterns observed in the excitatory population in absence and presence of gap junction, respectively. Secondly, we further report these similar network states again, showing features of robustness with network densities. Our results imply that, in excitatory-inhibitory balance networks, gap junction and weights of chemical synaptic connections together can make a great contribution to generate various spatiotemporal patterns.

2 Models and methods

2.1 Neuronal dynamics

Wang-Buzsáki model. The Wang-Buzsaki model [88, 89]resembles the dynamics of fast-spiking neurons in the cortex and hippocampus, and it is used here only as a general model of mammalian neuronal excitability. The Wang-Buzsáki model has three state variables for each neuron: membrane potential V, the Sodium inactivation variable h and Potassium activation variable n, corresponding to the spike-generating Na^+ and K^+ voltage-dependent ion currents (I_{Na} and I_K), respectively. Sodium activation variable m is considered to be instantaneous. The neuronal dynamics is as :

$$\begin{aligned} C_m\frac{dV}{dt} &= -I_{Na} - I_K - I_L - I_{Syn} \\ \frac{dh}{dt} &= \phi(\alpha_h(1-h) - \beta_h h) \\ \frac{dn}{dt} &= \phi(\alpha_n(1-n) - \beta_n n) \end{aligned} \tag{1}$$

where $I_L = g_L(V - E_L)$, $I_{Na} = g_{Na}m_\infty^3 h(V - E_{Na})$ and $I_K = g_K n^4(V - E_K)$ represent the leak currents, transient sodium current and the delayed rectifier current, respectively. I_{syn} stands for the synaptic current (in $\mu A/cm^2$). The parameters g_L, g_{Na}, g_K are the maximal conductance density, E_L, E_{Na}, E_K are the reversal potential and $m_{\infty_{(v)}}$ is the steady-state activation variable m of the Hodgkin-Huxley type [90].

In the simulation, unless stated otherwise, the parameters and functions used are given in Table 1.

Synaptic dynamics. By applying the Wang-Buzsáki model to the nodes of the network that incorporates both types of synapses, neurons in the network are connected by electrical (linear diffusive coupling) and chemical (nonlinear coupling) synapses. The total synaptic input currents into neuron i within excitatory population, is given by:

$$I_{SynE,i} = J_{gap}\sum_{j=1,j\neq i}^{N_E} C_{gap}^{ij}(V_i - V_j) + J_{EE} \sum_{j=1,j\neq i}^{N_E} L_{EE}^{ij} g_{syn,j}(V_i - E_{synE})$$

Table 1 Parameters and functions of Wang-Buzsáki model(1996) [88]

$g_L = 0.1$	$g_{Na} = 35$	$g_K = 9\ (mS/cm^2)$
$E_L = -65$	$E_{Na} = 55$	$E_K = -90$ (mV)
$C_m = 1\ (\mu F)$	$\phi = 5$	$I_{app} = 0\ (\mu A/cm^2)$
$\alpha_m(V) = -0.1(V+35)/[exp(-0.1(V+35))+1]$		$\beta_m(V) = 4exp[-(V+60)/18]$
$\alpha_h(V) = 0.07exp[-(V+58)/20]$		$\beta_h(V) = 1/exp[-0.1(V+28)]+1$
$\alpha_n(V) = -0.01(V+34)/[exp(-0.1(V+34))-1]$		$\beta_n(V) = 0.125exp[-(V+44)/80]$
$m_\infty = \alpha_m/(\alpha_m+\beta_m)$		

$$+ J_{EI} \sum_{j=1, j\neq i}^{N_I} L_{EI}^{ij} g_{syn,j}(V_i - E_{synI}) + \sum_{i=1}^{N_E} g_{syn,j}(V_i - E_{synE}) \quad (2)$$

The four terms on right-hand side of Eq. (2) corresponds to electrical synaptic inputs, self-excitatory synaptic inputs, inhibitory synaptic inputs (from inhibitory population) and external excitatory synaptic input to each neuron in the excitatory population, respectively. The connection matrices C_{gap}^{ij}, L_{EE}^{ij}, L_{EI}^{ij} are described in the network connectivity section. Lastly, purely chemical synaptic input currents for inhibitory population is as follows:

$$I_{SynI,i} = J_{II} \sum_{j=1, j\neq i}^{N_I} L_{II}^{ij} g_{syn,j}(V_i - E_{synI}) + J_{IE} \sum_{j=1, j\neq i}^{N_E} L_{IE}^{ij} g_{syn,j}(V_i - E_{synE}) \quad (3)$$

The two terms on right-hand side of Eq. (3) represent self-inhibitory synaptic input and excitatory synaptic inputs (from excitatory population).

We use a second-order differential equation to model chemical synaptic conductances g_{syn} [91,92], provided by:

$$\frac{d^2 g_{syn}}{dt^2} = \bar{g}_{s(E,I,\nu)} f \delta(t_0 + t_d - t) - \left(\frac{1}{\tau_1} + \frac{1}{\tau_2}\right)\frac{dg_{syn}}{dt} - \frac{g_{syn}}{\tau_1 \tau_2} \quad (4)$$

The delta function $\delta(t_0 + t_d - t)$ represents the spike signal from presynatpic cell, that is 1 when $t = t_0 + t_d$ and 0 otherwise. The time t_0 is the time of the presynaptic spike and t_d is the synaptic delays from the presynatpic to postsynaptic cell. The conductance peaks occurs at time $t_{peak} = t_0 + t_d + \frac{\tau_1\tau_2}{\tau_1 - \tau_2} ln(\tau_1/\tau_2)$. The normalization factor f ensures that the maximum amplitude of the impulse response equals $\bar{g}_{s(E,I,\nu)}$,

$$f = \frac{1}{e^{-t_{peak}/\tau_1} - e^{-t_{peak}/\tau_2}}$$
$$t_{peak} = \frac{\tau_1\tau_2}{\tau_1 - \tau_2} ln(\tau_1/\tau_2) \quad (5)$$

In simulations and for practical reasons, second order differential equations are solved as follows:

$$\frac{dy}{dt} = \bar{g}_{s(E,I,\nu)} f \delta(t_0 + t_d - t) - \left(\frac{1}{\tau_1} + \frac{1}{\tau_2}\right) y - \frac{g_{syn}}{\tau_1\tau_2}$$
$$\frac{dg_{syn}}{dt} = y \quad (6)$$

In simulations, both peak synaptic conductances $\bar{g}_{s(E,I,\nu)}$ and synaptic delays t_d are Gaussian distributed random variables with prescribed means $g_{s(E,I)}$ and $\overline{D}$, and standard deviation $\sigma_{g_{s(E,I)}}$ and $\sigma_{\overline{D}}$. The background drive v_{ext} to each neuron in the excitatory population was provided by external excitatory inputs, modeled as independent and identically distributed Poisson processes with rate ν for different neurons. Peak conductances of the external drive were also heterogeneous and assumed values sampled from a truncated Gaussian distribution with mean $g_{s\nu}$ and standard deviation $\sigma_{g_{s\nu}}$. These rules are the same as the previous study [89]. Parameters of synaptic model are summarized in Table 2.

Table 2 List of simulation and default network parameters in the E/I balanced networks

A: Global simulation paramters		
Description	**Symbol**	**Value**
Simulation duration	T_{sim}	2000 ms
Start-up transient	T_{trans}	400 ms
Time step	dt	0.01 ms
B: Populations and external input		
Description	**Symbol**	**Value**
Population size of excitatory neurons	N_E	1000
Population size of inhibitory neurons	N_I	250
Possion input rate (external excitatory inputs)	ν	6000 Hz
C: Connection parameters		
Description	**Symbol**	**Value**
Weight of gap junction	J_{gap}	0.1
Weight of self-excitatory connection	J_{EE}	0.05
Weight of self-inhibitory connection	J_{II}	0.04
Weight of inhibitory connections for excitatory population	J_{EI}	0.03
Weight of excitatory connections for inhibitory population	J_{IE}	0.01
Probability of local inhibitory connections	P_I	0.2
Synaptic dynamics (Difference of Two Exponentials)		
Reversal potential for excitatory synapses	E_{synE}	0 mV
Reversal potential for inhibitory synapses	E_{synI}	-80 mV
Excitatory synaptic decay time	τ_{1E}	3 ms
Ihibitory synaptic decay time	τ_{1I}	4 ms
Excitatory synaptic time	τ_{2E}	1 ms
Inhibitory synaptic time	τ_{2I}	1 ms
Mean synaptic delay	$\overline{D}$	1.5 ms
Mean synaptic excitatory conductance	g_{sE}	5 nS
Mean synaptic inhibitory conductance	g_{sI}	200 nS
Mean synaptic input conductance	g_{sv}	3 nS
Standard deviation delay	$\sigma_{\overline{D}}$	0.1 ms
Standard synaptic excitatory conductance	$\sigma_{g_{sE}}$	1 nS
Standard inhibitory conductance	$\sigma_{g_{sI}}$	10 nS
Standard input conductance	$\sigma_{g_{sv}}$	1 nS
Small-world networks (SW)		
Probability of replacing new links	P_{sw}	0.01
Degree of nearest neighbours connections	K	10

2.2 Network connectivity

To build the connectivity matrix, we consider a balanced neural network, consisting of $N_E = 1000$ excitatory and $N_I = 250$ inhibitory neurons (Fig. 1). The excitatory population itself is connected by excitatory synapses in small world topology and its adjacent neurons are also connected by gap junctions. The inhibitory population itself is connected all-to-all by inhibitory synapses. The matrix L_{kl}^{ij} denotes the connections between the ith neurons of the kth population and the jth neurons of the lth population. For example, the matrix of self-excitatory (or self-inhibitory) connections is defined as L_{EE}^{ij} (or L_{II}^{ij}), while the all-to-

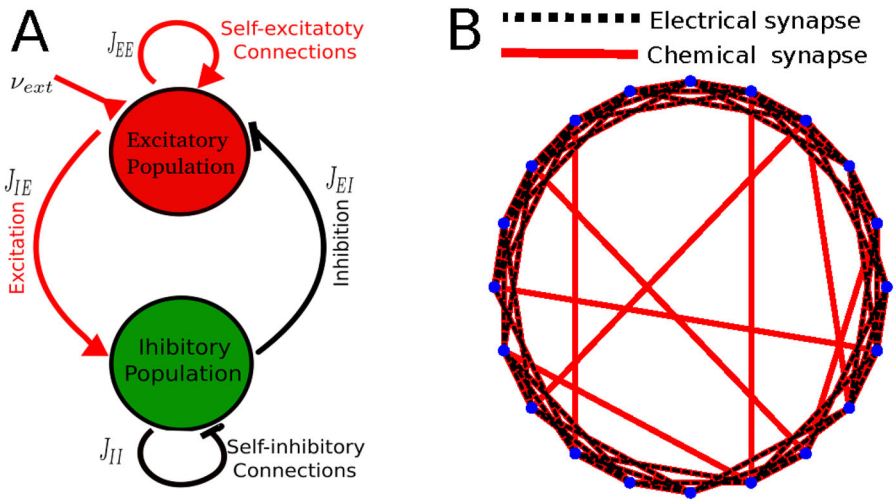

Fig. 1 Network architecture and parameters. **A**. The balanced neural networks containing excitatory (*red*) and inhibitory population (*green*). The synaptic input (excitatory synaptic input or inhibitory synaptic input) between the populations are generated by all-to-all connections. Their coupling strength between the populations is denoted with constants J_{IE} and J_{EI}. Self-inhibitory connections (of the weights J_{II}) is all to all connections. Excitatory (inhibitory) connections are represented in red (*black*). ν_{ext} is the external drive to each neuron in the excitatory population by external excitatory inputs. **B**. Diagram of excitatory population, which is connected by excitatory synapses (with weights J_{EE}, *red solid lines*) in a small world topology and adjacent neurons are also connected by electrical synapses (with weights J_{gap}, *black dashed lines*). We fix $J_{II} = 0.04$, $J_{IE} = 0.01$. (Color figure online)

all matrix of excitatory-to-inhibitory (or inhibitory-to-excitatory) population connections is L^{ij}_{IE} (or L^{ij}_{EI}). The parameters J_{EE} , J_{II} and J_{IE} (or J_{EI}) stand for corresponding weights of self-excitatory connections, self-inhibitory connections and excitatory-to-inhibitory (or inhibitory-to-excitatory) population connections. Here $L^{ij}_{kl} = 1$ (or 0) corresponds to connections between neuron i and j (or not). Besides, the matrices of adjacent connections by electrical synapses in excitatory population is C^{ij}_{gap} with corresponding coupling strengths J_{gap}. The default network parameters used are shown in Table 2.

The small-world topology mentioned above is implemented as two basic steps of the standard algorithm [93]: 1. Construct a regular ring lattice with N nodes of mean degree $2K$. Each node is connected to its K nearest neighbors on either side. 2. For every node $i = 0, ..., N-1$ take every edge connecting i to its K rightmost neighbors – that is every edge $(i, j \bmod N)$ with $i < j \leq i + K$, and rewire it with probability P_{sw}. Rewiring is done by replacing $(i, j \bmod N)$ with (i, k) where k is chosen uniformly at random from all possible nodes.

2.3 Network activity characterization

In this paper we first use the **synchronization index** $\chi(N)$, previously introduced by Ref [94,95] , to account for the synchronization level of the neural activity of the considered networks, where:

$$\chi^2 = \frac{N\sigma^2_{V(t)}}{\sum_{i=1}^{N}\sigma^2_{V_i(t)}} \tag{7}$$

Here $V(t) = \frac{1}{N}\sum_{i=1}^{N} V_i(t)$ is population average of the membrane potential $V_i(t)$. The variables $\sigma_{V(t)}$ and $\sigma_{V_i(t)}$ denote the standard deviation of $V(t)$ over time, or of the membrane potential traces $V_i(t)$ of each isolated neuron i,respectively. χ is 1 when all the neurons have the same trajectory and 0 for an incoherent state when the fluctuations of $V(t)$ are 0.

To further investigate the global dynamical behavior of the neural networks, we then introduce the **order parameter** and its the variance in time, **metastability**. The order parameter R, describes the global level of phase synchrony in a system of N_E oscillators [96,97], given by:

$$R = \left\langle \left| \frac{1}{N_E} \sum_{k=1}^{N_E} e^{2\pi i[(t-t_k^n)/(t_k^{n+1}-t_k^n)]} \right| \right\rangle \quad (8)$$

where the vertical bars ($= \phi_c(t)$) denote the modulus of the complex number and the angle brackets is the temporal average, while the exponent, $2\pi[(t-t_k^n)/(t_k^{n+1}-t_k^n)]$, is the phase we assign to each neurons in the excitatory population. The closer to 0 (1) R becomes, the more asynchronous (synchronous) the dynamics is. N_E is the total number of excitatory population, t_k^n is the time of the nth spikes of neurons k and t_k^{n+1} is the time of the following $(n+1)$th spikes.

In order to quantify the metastability and chimera-likeness of the observed dynamics, the global metastability Met [98] , is the variance in time of order parameter R, by:

$$Met = \frac{1}{T} \sum_{t \leq \Delta t} (\phi_c(t) - R)^2 \quad (9)$$

where $T = T_{sim}$ in Eq. (9) is the whole simulation time to quantify the metastability of the excitatory population. Metastability is 0 if the system is either completely synchronized or completely desynchronized – a high value is present only when periods of coherence alternate with periods of incoherence.

3 Results

3.1 Influence of electrical coupling communicating excitatory neurons in the generation of several firing patterns

Networks with mixed excitatory/inhbitory (E/I) neurons, connected by chemical synapses, can display a variety of firing patterns depending on their E/I balance. Fig. 2A shows samples of raster plots (action potentials) and voltage traces resulting from the simulation of a network consisting on 1,000 excitatory and 250 inhibitory neurons, at different values of the E/I synaptic weights received by the excitatory population (J_{EE}, J_{EI}, see values in Figure Legend). We characterized these firing regimes by calculating the synchronization index $\chi(N)$ (Eq. 7) for the voltage traces, and the Kuramoto order parameter R for the phase synchronization based on the spike firing (see Eq. 8) for phase synchronization. We also introduce the metastability Met Eq. (9) to quantify the metastability and chimera-likeness of the observed dynamics within the excitatory population. Column a shows mostly incoherent firing, in spite the fact that inhibitory neurons are firing periodically and in synch. As the inhibitory weight is increased (b, c, d), we see that excitatory neurons not only fire less but they show a larger synchronization index, as has been largely reported [54–58,63]. Panel d goes further than the spike synchronization, showing also a high value of synchrony in the voltage traces. Increasing the excitatory weights, on the other hand, (e, with an inhibitory drive similar to c) causes the network to fire periodically but in this case we found the firing to be more irregular as evidenced by a higher metastability value.

Then, we simulated the same (J_{EE}, J_{EI}) combinations but in the presence of electrical synapses communicating the excitatory neurons in a lattice fashion, where each neuron is reciprocally connected to its 10 closest neighbors. Fig. 2B–D shows the effect of the electrical synapses on the firing patterns that were already described. In the first case (a), there is an emergence of traveling waves, something that can not be observed without gap junctions. These traveling waves show a tendency to synchronize and spread faster as the conductance of gap junction is increased (compare B,C and D). In the cases of synchronized firing (b,c) the introduction of electrical coupling further increases the synchrony producing a much more coherent activity also favoring total synchronization of the voltage time courses. This synchronization with oscillatory behavior occurs with period 2 (b) and 1 (c) depending on the degree of inhibition. In d we see that the combination of electrical coupling and stronger inhibition leads to suppression of spikes, giving rise to synchronized subthreshold oscillations. An interesting highly metastable behavior is found in the regime with higher excitatory level (e). The raster plots in row 3 ($J_{gap} = 0.05$) of column e show the appearance of disordered traveling waves that often take the form of chimera-like states, where two subpopulations coexist; one with synchronous activity and the other with ripple events. More importantly, chimera-like states are also metastable, meaning that they can stay in the vicinity of one stable state for a certain time interval and then, spontaneously move towards another. Again, the firing patterns in column e have a tendency to synchrony as electrical connections are increased but nevertheless they maintain a high metastability index. Thus, the introduction of gap junctions into the excitatory population can lead to a new variety of firing patterns (wave propagation, synchronized oscillations, chimera-like

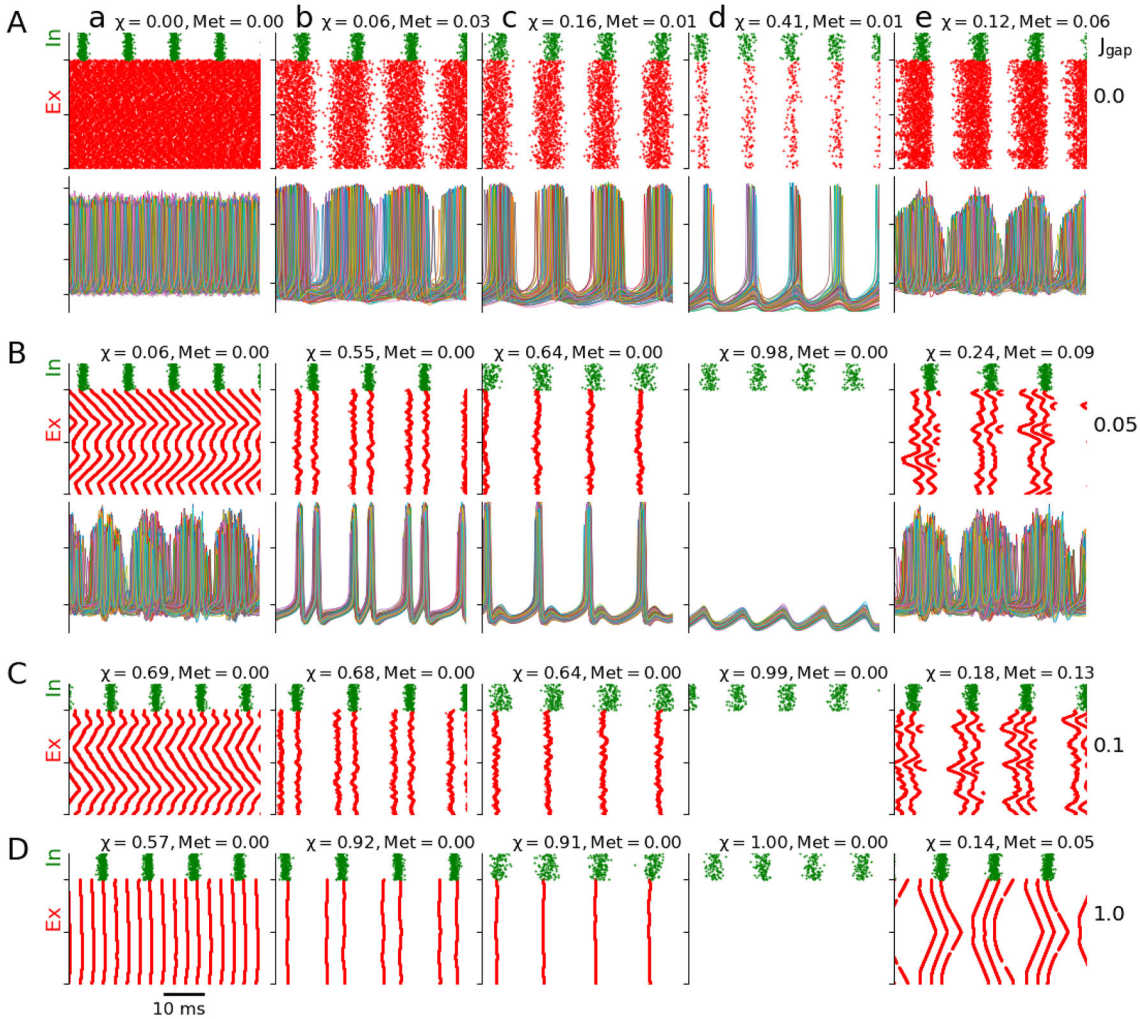

Fig. 2 **A**. Samples of raster plots and voltage traces of network purely connected by chemical synapses. **B-D**. Samples of raster plots in the same (J_{EE}, J_{EI}) combinations but in presence of electrical synapses communicating the excitatory neurons when $J_{gap} = 0.05, 0.1, 1.0$, respectively. The voltage traces are shown below each raster plot in **B**. Values of (χ, Met) pairs are shown upper each raster plot. Values of (J_{EE}, J_{EI}) combinations are: a:(1.1, 0.045), b:(0.48, 0.16), c:(0.5, 0.35), d:(0.8, 0.82), e:(2.4, 0.40). The red Ex (green In) indicate index of excitatory population (inhibitory population). The scale bars for all subplots is 10 ms.The presence of a dot in a raster plot, indicates that the neuron whose index corresponds to that row produced an action potential (spike) at the time corresponding to that column. For raster plot and voltage traces calculation, simulations were solved with both Euler method and fourth-order Runge-Kutta scheme with integration time step $dt = 0.01$ written in Python. No detectable differences were found between these two methods. Data analysis and plotting was performed with Python and the libraries Numpy, Scipy, and Matplotlib. (Color figure online)

and metastable state) that cannot be induced solely by chemical synapses.

In order to appreciate better the effects of electrical coupling on network dynamics, we swept a full region of the J_{EE}, J_{EI} parameter space, characterizing the behavior of the network by means of the previously mentioned synchrony and metastability indexes. The results from a network connected solely by chemical synapses is shown in 3A. The letters *a-e* represent the location of the raster plots and voltage traces shown in Fig 2. As widely reported before [54–58,63] the general synchronization index χ is highly dependent on the strength of inhibitory connections, showing a graded increase from top to bottom. The synchroniza-

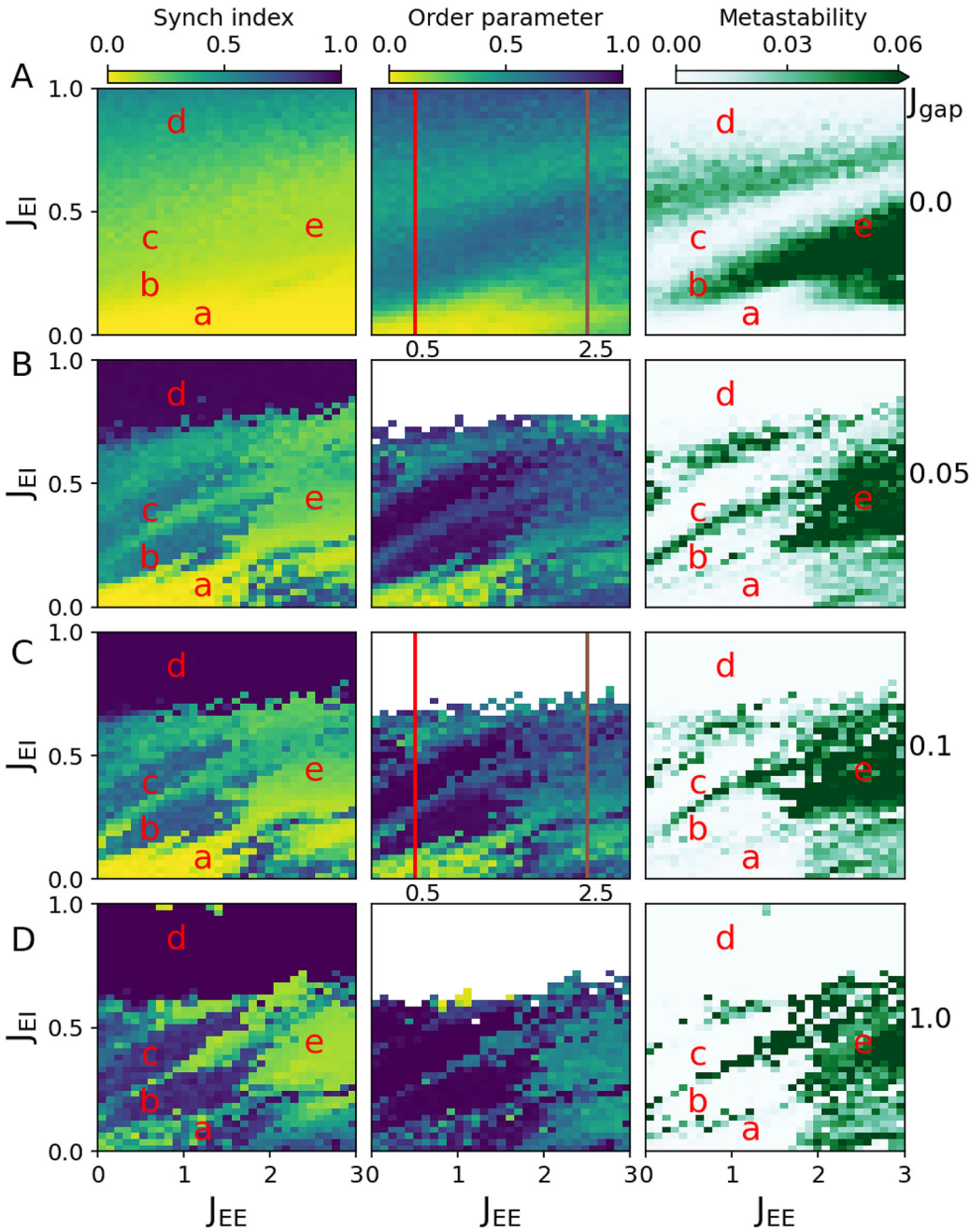

Fig. 3 The effect of electrical coupling on firing patterns of excitatory neurons in J_{EE}/J_{EI} parameter space. **A**.Collective dynamics behavior of excitatory neurons connected by purely chemical synapses. (a-c) Incoherent state; (d)Metastable state; (e) Generalized synchronous state. **B–D**. Significant emergence of neural network state in presence of electrical coupling between excitatory neurons. (a) Traveling wave ; (b,c) Synchronous states; (d) Metastable state or chimera-likeness;(e) Subthreshold synchronous states. The electrical synaptic weights for each subplot are **B.** $J_{gap} = 0.05$, **C.** $J_{gap} = 0.1$, **D.** $J_{gap} = 1$

tion of spikes, that we measure with the Kuramoto's order parameter R, shows a similar pattern although the synchronized region appears less homogeneous than in the case of the general index χ. The metastability index also shows this, with a metastable region separating the synchrony regions c and d. As hinted by Fig. 2, an increase in the excitation strength causes the appearance of a region with higher metastability (e) in the first transition from asynchronous to synchronous firing.

The effect of electrical coupling between excitatory neurons is appreciated in Fig. 3B–D. There is a dramatic increase in the synchrony measures although this effect is not evenly distributed across the whole parameter space. Some regions show a high increase in synchrony (b,c) but they get separated by an intermediate synchrony region, and this intermediate region is also characterized by high metastability (more on this later). Other regions (a) show a gradual increase in synchrony, as if their dynamics was less susceptible to electrical coupling. Nevertheless, a high synchrony regime is reached with the maximal conductance J_{gap}. As shown in Fig. 2 (column a), this region is characterized by traveling waves of activity that do not show metastable behavior. The region containing the d point, looses the spiking activity and falls into a subthreshold oscillatory regime readily with the lowest J_{gap} value. As the electrical coupling conductance is increased, this region grows and is seen at progressively lower values of the inhibitory strength J_{EI}. Finally, the region e remains the same (in terms of synchrony) regardless of the presence of electrical coupling and its conductance value. This is striking, as Fig. 2 already showed a dramatic change in the firing patterns that are thus not captured by the global behavior indexes χ, R and Met. Looking at the firing patterns, we can see that the most important difference is the spatial organization of the irregular and metastable firing activity.

In summary, two significant results are observed in the previous simulations. Firstly, we found that networks of excitatory neurons solely connected by chemical synapses, can exhibit a variety of firing patterns depending on their E/I balance. Secondly, we further found that the introduction of gap junctions into the excitatory population can cause a new variety of firing patterns, such as traveling wave, synchronized oscillations, chimera-like and metastable state that can not be induced solely by the chemical synapses.

In the following, we will examine in more detail the transitions between the firing regimes caused by the increase in inhibitory strength. To do this, we will focus in two values of excitatory strength: $J_{EE} = 0.5$, roughly sweeping the areas near a-d, and $J_{EE} = 2.5$, that contains the e point.

3.2 The transitions between different firing regimes

We investigated the various firing patterns at a fixed excitatory level $J_{EE} = 0.5$, to characterize the transitions between the firing patterns represented by a to d in Fig. 2. Fig. 4 shows the evolution of the synchrony R and Metastability as J_{EI} is swept from 0 to 1.0; in absence (Fig. 4A,C) and presence (Fig. 4B,D) of electrical coupling.

In the absence of electrical coupling (Fig. 4A, C), the network reaches some degree of synchrony at $J_{EI} \approx 0.15$ however full synchrony is never observed. The activity is mostly incoherent, with varying values of R and Met. Some regimes can be defined based on the different values of Met but they don't appear much different and the transition between them is smooth. In contrast, the presence of electrical coupling (Fig. 4B, D) produces the appearance of clearly synchronized states as well as the already mentioned traveling waves pattern when $J_{EI} < 0.1$. The finer sweep of the inhibitory strength now allows to observe that the transition between the two-spike firing pattern (2) and the one-spike pattern (4) occurs with a more disordered pattern (3), characterized by high metastability and the existence of unstable and transient traveling waves. Unstable traveling waves appear again ((5) and (6)) in the transition to the non-firing oscillatory regime when $J_{EI} > 0.5$. It is evident that the inhibitory level J_{EI} is a significant system parameter which plays a major role in determining the emergence of the above mentioned firing patterns, including traveling wave, synchrony state with one-spike (or two-spike), a peculiar chimera-likeness behavior and subthreshold synchronous states. More importantly, there are transitions between dynamical states depending on the inhibitory level among individual neurons.

We repeated the same exploration at a higher level of excitatory strength, $J_{EE} = 2.5$ (Fig. 5), therefore characterizing the e point in Fig. 2. Both in absence (Fig. 5A, C) and presence (Fig. 5B, D) of electrical coupling,

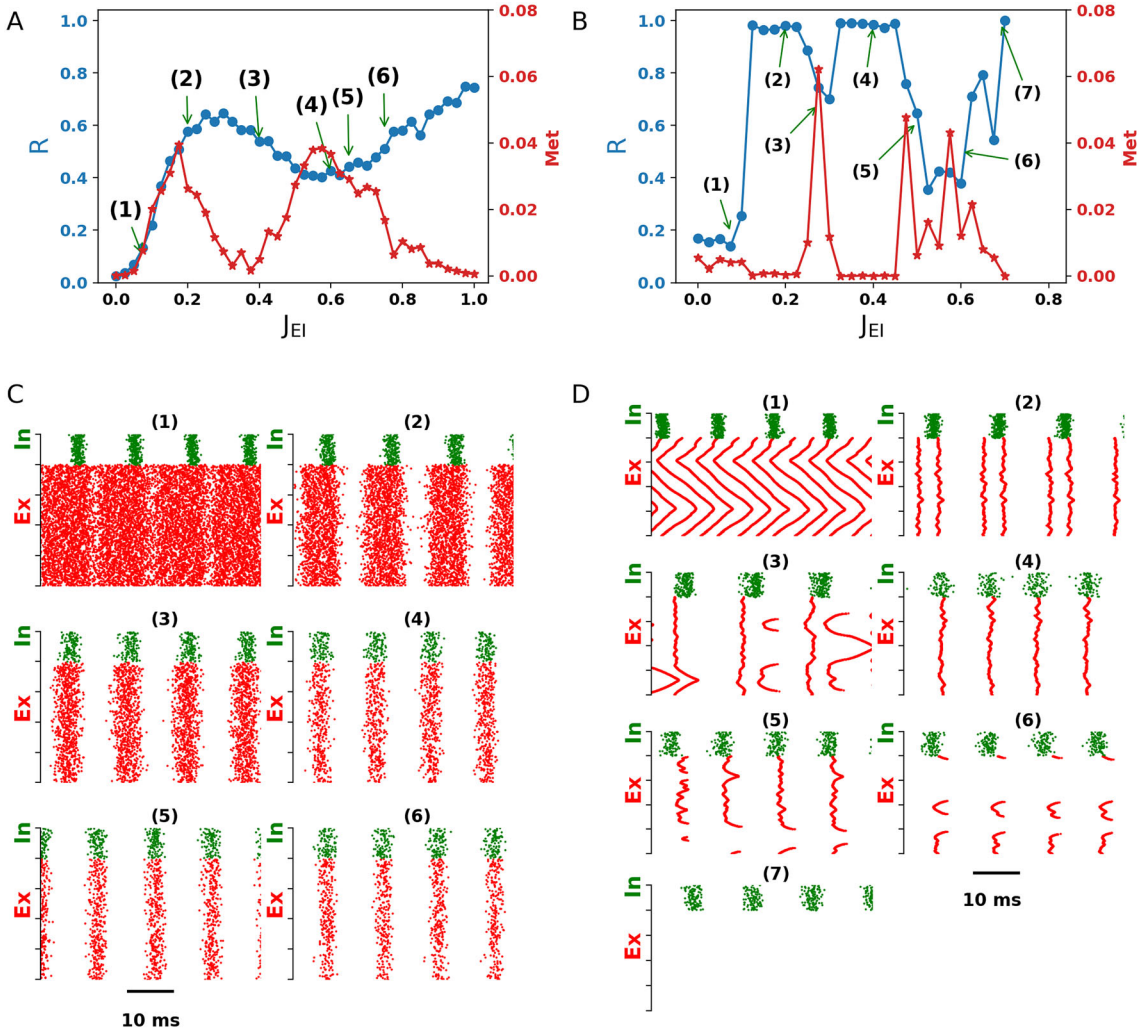

Fig. 4 Influence of the inhibitory level J_{EI} on the emergence of spatiotemporal dynamical states in absence(**A** and **C**. $J_{gap} = 0$) and presence of (**B** and **D**. $J_{gap} = 0.1$) electrical coupling where $J_{EE} = 0.5$. The emergence of collective dynamics in the excitatory population quantified by the order parameters (*blue circle lines*) and metastability (*red star lines*). **C** and **D** show a detail of the typical spatiotemporal firing patterns in each dynamics regimes of sweeping parameter J_{EI}. (Color figure online)

the firing patterns that we observe are much more disordered than in the previously explored case. Without gap junctions, the network always shows a somewhat incoherent firing, although synchrony increases with the inhibitory strength.

In contrast, the presence of electrical coupling (Fig. 5D) produces firing patterns that are much more structured without being fully synchronized. Three different types of neuronal activity in the excitatory population can be recognized. There is a much more regular population activity, for weak inhibitory synaptic connections. The range of J_{EI} becomes narrower for traveling waves and wider for chimera-like state with increasing excitability levels that are shown in Fig. 3D. Traveling waves vanish at very high excitability levels, similar to a previous study [87]. If the inhibitory coupling strength is sufficiently increased among range $0.25 < J_{EI} \leqslant 0.7$ where both R and Met are high, we observe chimera-like behavior. In addition, we also see metastable states that alternate between synchronous

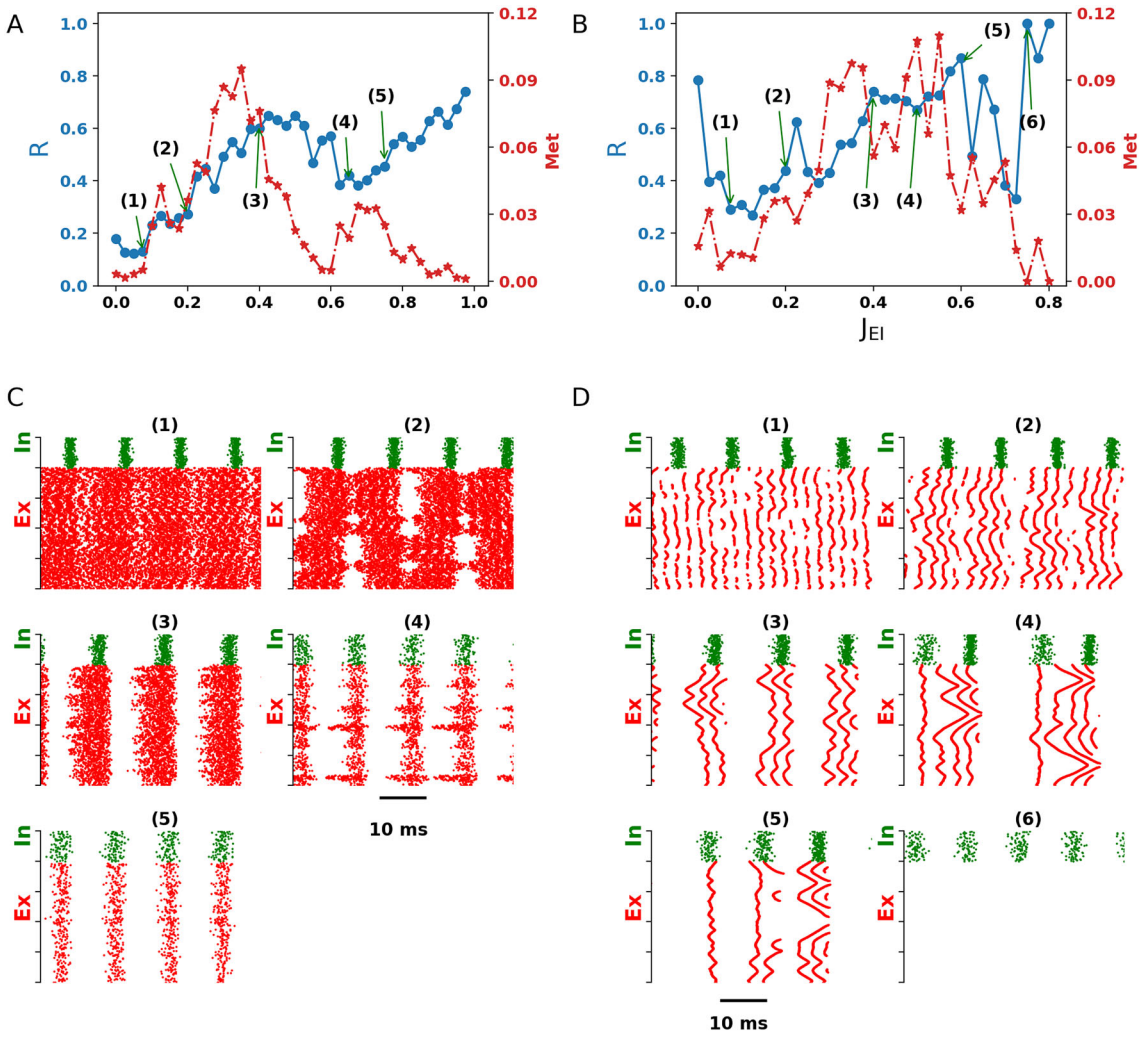

Fig. 5 Distinct types of dynamical behavior as J_{EI} varies as illustrated in **A** ($J_{gap} = 0$) and **B** ($J_{gap} = 0.1$) but with high excitatory level where $J_{EE} = 2.5$. **C** and **D** present typical firing patterns of these two cases in each dynamics regimes

and incoherent behaviors with different time windows. If J_{EI} is further increased ($J_{EI} > 0.7$), spiking ceases and instead subthreshold oscillations (without spikes) emerge.

3.3 Effect of electrical connections in a different chemical synapse topology

To present a broader perspective on variety of firing patterns in presence of electrical coupling among excitatory neurons, and understand its robustness under well-defined assumptions, we choose a higher probability P_{sw} ($= 0.5$) of rewiring excitatory connections, resulting in a network closer to a random topology rather than small-world connectivity. Fig. 6 characterizes the collective behavior of excitatory neurons in absence (Fig. 6A) and presence (Fig. 6B–D) of electrical coupling on (J_{EE}, J_{EI}) plane. It is clear that the similar firing patterns have been observed in this case, emerging as five different dynamical regimes that were already mentioned in Fig. 3. In order to better reveal these firing pattern in each dynamical regimes, Fig. 7 shows samples of raster plots of excitatory neurons in absence (A) and presence (B–D) of electrical coupling. Introduction of electrical coupling still induces a variety of firing pattern shown in Fig. 7B–D , such

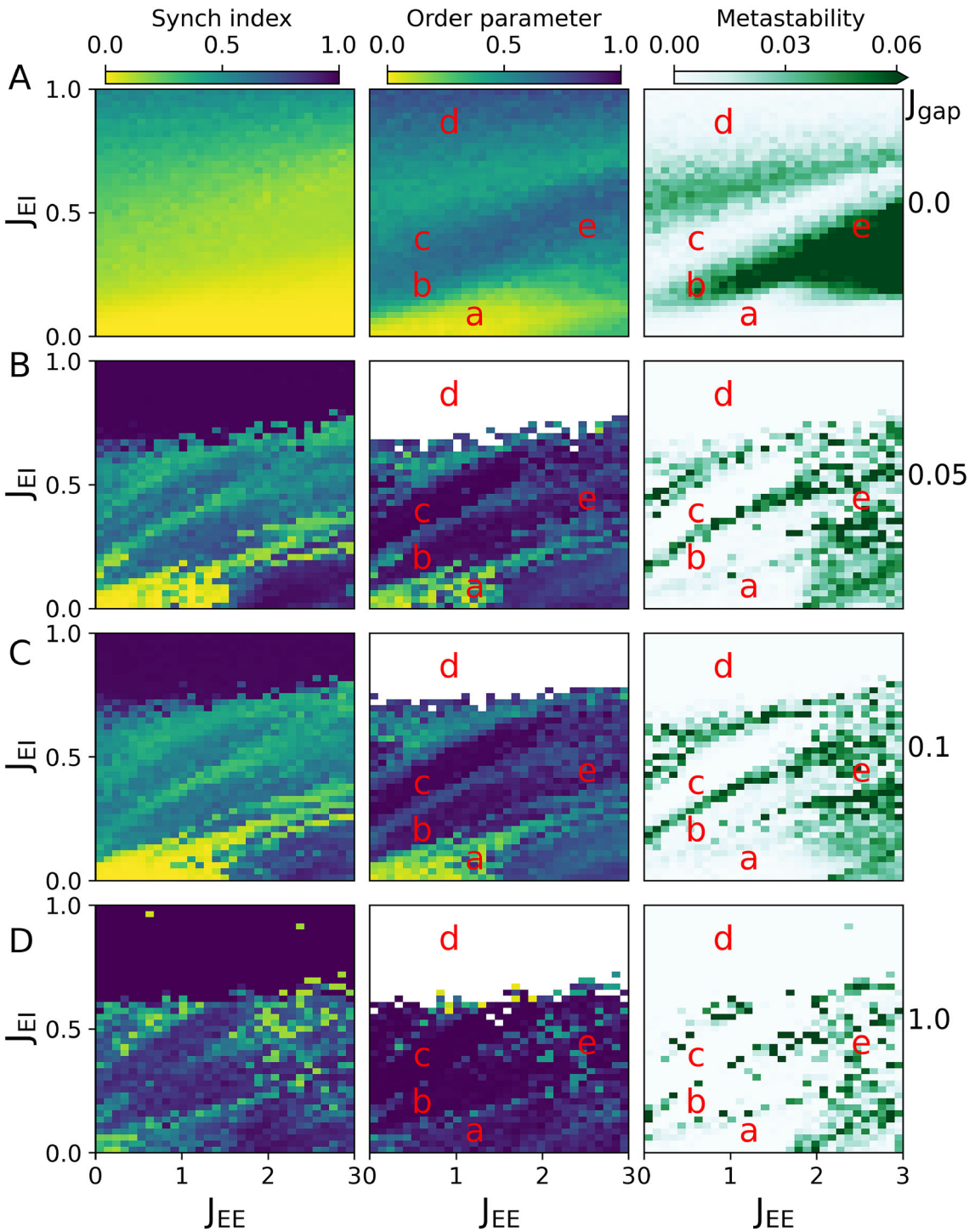

Fig. 6 The effect of electrical coupling on dynamical regimes of spatiotemporal firing patterns when $P_{sw} = 0.5$, showing the similar dynamical behavior and a good robustness effect under a clear comparison with Fig. 3. **A**.Collective dynamics behavior of excitatory neurons connected by purely chemical synapses. (a–c) Incoherent state; (d)Metastable state; (e) Generalized synchronous state. **B**–**D**. Significant emergence of neural network state in presence of electrical coupling between excitatory neurons. (a) Traveling wave ; (b,c) Synchronous states; (d) Metastable state or chimera-likeness;(e) Subthreshold synchronous states

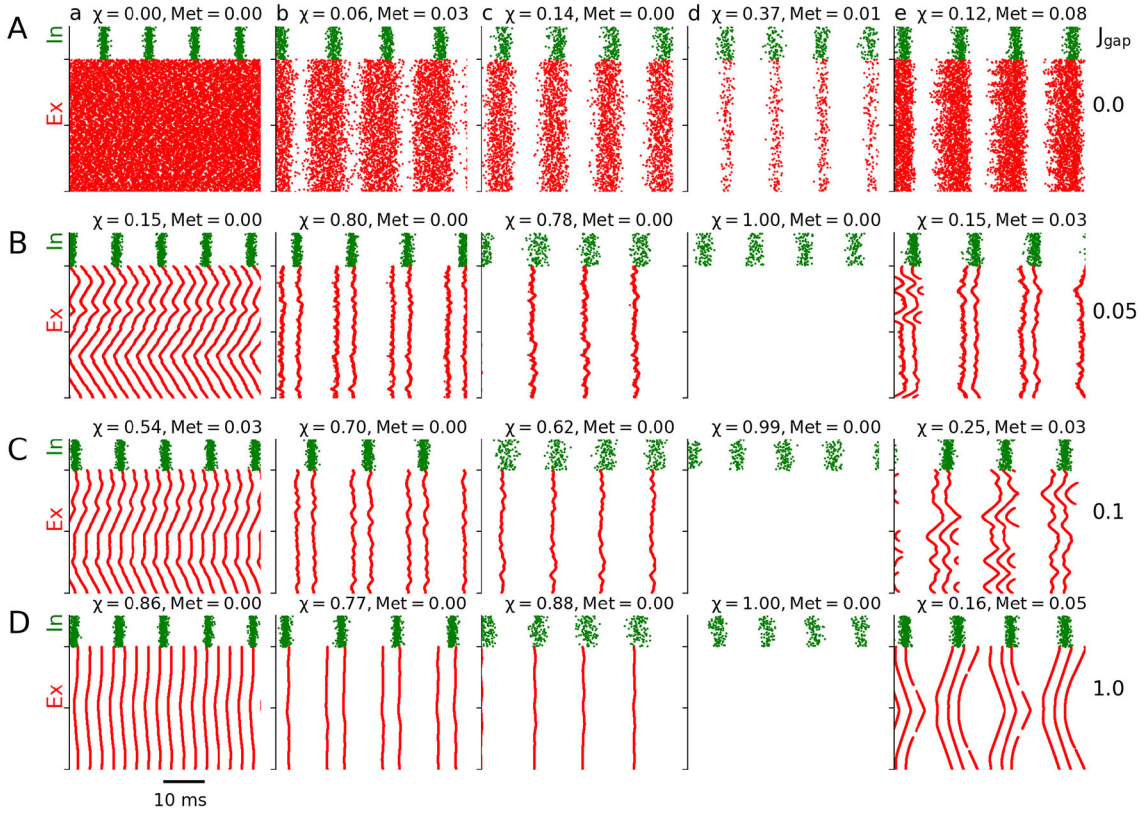

Fig. 7 Samples of raster plots of E/I neuronal network both in absence (**A**) and presence of (**B–D**) electrical synaptic connections among excitatory neurons when $P_{sw} = 0.5$, the other parameters are the same as Fig.2

as traveling waves, two types of synchronous states, chimera-like (or metastable state) with various ripples events, and subthreshold synchronous states. By changing parameters such as weights of gap junction and inhibitory connections, the way of synaptic connections per excitatory neurons, we observed these similar network states again, showing features of robustness with network densities. Similarly, we found our results to be robust with respect to the values of J_{II} and J_{IE}, obtaining the same effect of electrical synapses as long as the excitation/inhibition balance is conserved.

To sum up, using statistical measurement of synchronization index, order parameter and metastability, we found that excitatory neurons connected by both chemical and electrical synapses of E/I balance network, can display various types of different levels of synchronous activity, implying vastly different computational properties. For weak excitatory coupling, the excitatory population displays rich collective dynamics – traveling waves, two-spike (or one-spike) synchrony firing pattern, metastable state, chimera-likeness (or metastable state) and lastly oscillation without spikes – as inhibitory level J_{EI} varies. However, for strong excitatory couplings, we found that the increasing inhibitory level J_{EI} in the networks of excitatory population only leads to three fundamentally different types of neuronal activity, namely, less regular population activity, chimera-like behavior (or metastable state) and subthreshold synchronous states (oscillation without spikes).

4 Discussion

In this paper, we investigated how electical synapses among excitatory (pyramidals) cells can affect collective dynamics of E/I balanced networks. While several works have focused on electrical synapses among cortical interneurons experimentally and their functional roles by both computational neuroscientist and exper-

imentalists, few studies have explored the impact of synaptic connections among pyramidal cells to neural networks. Experimental evidence for the similar junctions in the cortex has, however, remained elusive due to the apparent rarity of these coupling among excitatory neurons. An interesting study by Jennifer et al [99]. has shown that the presence or absence of pairwise ES-coupled neurons does little to influence global network behavior, the ES-coupled excitatory neurons themselves, however, only exhibit pair-wise synchrony and oscillations.

With the goal of understanding what role of electrical communication between excitatory cells might play in influencing network dynamics, we systematically swept the connection parameters of synaptic weights, trying to keep other variables, such as parameters of synaptic dynamics. At first glance, our results are not as straightforward to interpret as in the previously mentioned works [43,85–87,100,101].This is not surprising, as various synchrony firing events arises in networks purely connected by electrical or chemical synapses together with synaptic weights and seems to depend on other factors such as time delay and networks topology. However, we found that the whole excitatory population has a tendency to synchronization as the weights of ES-coupling among excitatory cells are increased. Moreover, the existence of these ES-connections can cause a new various firing patterns of interest (such as synchronous firing, various ripples events) by slightly changing the chemical synaptic weights, that can not be induced by solely synaptic connections.

Since we have shown that ES-coupled excitatory cells can allow for significant neural firing changes in the network dynamics due to addition of electrical synapses, we next further investigated that chemical synaptic inhibition from inhibitory neurons to ES-coupled excitatory population are enhanced. In this case, we showed that the variation of this inhibition can induce more than 5 firing patterns with different timescale ripples events at weaker excitatory level. More importantly, the increasing inhibition does not simply result in the similar firing modes at stronger excitatory level, but instead results in the excitatory population with three fundamental firing patterns compared to those studies that do not (see [18–21]) . These simulation finding imply that addition and variation of inhibition in networks induce various firing patterns due to generating nonlinear effects. In other words, in the absence of inhibition, any type of external input would generate more or less the same one-way patterns.

Brain dynamics is often inherently variable and unstable, consisting of sequences of transient spatiotemporal patterns [102,103]. These sequences of transients are a hallmark of metastable dynamics that are neither entirely stable nor completely unstable. Our results pave a possible way to uncover the underlying mechanisms of generating metastable dynamics, such as chimera-likeness, that may mediate perception and cognition.

Acknowledgements We thank the funding No.4111190017 from Jiangsu University(JSU), China, and Fondecyt Project Nos.3170342 (K.X.), 21191760 (J.P.M.) and 1181076 (P.O.) from ANID, Chile. P.O. is partially funded by the Advanced Center for Electrical and Electronic Engineering (ANID FB0008, Chile). The Centro Interdisciplinario de Neurociencia de Valparaíso (CINV) is a Millennium Institute supported by the ANID grant ICN09-022.

Data Availibility Statement The datasets analysed during the current study are available in the github repository at https://github.com/keshengxuu/DiversiryFiringPatterns.

Declarations

Conflict of interest The authors declare that they have no conflict of interest.

References

1. Elson, R.C., Selverston, A.I., Huerta, R., Rulkov, N.F., Rabinovich, M.I., Abarbanel, H.D.I.: Synchronous behavior of two coupled biological neurons. Phys. Rev. Lett. **81**(25), 5692–5695 (1998)
2. Jing, J.: Network Functions and Plasticity: Perspectives from Studying Neuronal Electrical Coupling in Microcircuits. Academic Press, Cambridge (2017)
3. Coombes, S.: Large-scale neural dynamics: simple and complex. NeuroImage **52**(3), 731–739 (2010)
4. Muller, L., Chavane, F., Reynolds, J.: Cortical travelling waves: mechanisms and computational principles. Nat. Rev. Neurosci. **19**(5), 255–268 (2018)
5. Ma, J., Song, X., Tang, J., Wang, C.: Wave emitting and propagation induced by autapse in a forward feedback neuronal network. Neurocomputing **167**, 378–389 (2015)
6. Wang, Q.Y., Lu, Q.S., Chen, G.R.: Ordered bursting synchronization and complex wave propagation in a ring neuronal network. Phys. A Stat. Mech. Appl. **374**(2), 869–878 (2007)
7. Xu, K., Huang, W., Li, B., Dhamala, M., Liu, Z.: Controlling self-sustained spiking activity by adding or removing one network link. EPL (Europhys. Lett.) **102**(5), 50002 (2013)

8. Xu, K., Zhang, X., Wang, C., Liu, Z.: A simplified memory network model based on pattern formations. Sci. Rep. **4**(7568), 1–8 (2014)
9. De Zeeuw, C.I., Hoebeek, F.E., Bosman, L.W.J., Schonewille, M., Witter, L., Koekkoek, S.K.: Spatiotemporal firing patterns in the cerebellum. Nat. Rev. Neurosci. **12**(6), 327–344 (2011)
10. Tian, C.H., Zhang, X.Y., Wang, Z.H., Liu, Z.H.: Diversity of chimera-like patterns from a model of 2d arrays of neurons with nonlocal coupling. Front. Phys. **12**(3), 128904 (2017)
11. Huo, S., Tian, C., Kang, L., Liu, Z.: Chimera states of neuron networks with adaptive coupling. Nonlinear Dyn. **96**(1), 75–86 (2019)
12. Pereda, A.E.: Electrical synapses and their functional interactions with chemical synapses. Nat. Rev. Neurosci. **15**(4), 250–263 (2014)
13. Alcami, P., Pereda, A.E.: Beyond plasticity: the dynamic impact of electrical synapses on neural circuits. Nat. Rev. Neurosci. **20**(5), 253–271 (2019)
14. Sheng, M., Sabatini, B., Sudhof, T. (eds.): The Synapse. Cold Spring Harbor Laboratory Press, New York (2012)
15. Bennett, M.V.L., Zukin, R.S.: Electrical coupling and neuronal synchronization in the mammalian brain. Neuron **41**(4), 495–511 (2004)
16. Buzsaki, G.: Rhythms of the Brain. Oxford University Press, Oxford (2006)
17. Isaacson, J.S., Scanziani, M.: How inhibition shapes cortical activity. Neuron **72**(2), 231–243 (2011)
18. Anderson, J.S., Carandini, M., Ferster, D.: Orientation tuning of input conductance, excitation, and inhibition in cat primary visual cortex. J. Neurophysiol. **84**(2), 909–926 (2000)
19. Atallah, B.V., Scanziani, M.: Instantaneous modulation of gamma oscillation frequency by balancing excitation with inhibition. Neuron **62**(4), 566–577 (2009)
20. Wehr, M., Zador, A.M.: Balanced inhibition underlies tuning and sharpens spike timing in auditory cortex. Nature **426**(6965), 442–446 (2003)
21. Poo, C., Isaacson, J.S.: Odor representations in olfactory cortex: "sparse" coding, global inhibition, and oscillations. Neuron **62**(6), 850–861 (2009)
22. van Vreeswijk, C., Sompolinsky, H.: Chaos in neuronal networks with balanced excitatory and inhibitory activity. Science **274**(5293), 1724–1726 (1996)
23. Bittner, S.R., Williamson, R.C., Snyder, A.C., Litwin-Kumar, A., Doiron, B., Chase, S.M., Smith, M.A., Byron, M.Y.: Population activity structure of excitatory and inhibitory neurons. PLoS One **12**(8), 1–27 (2017)
24. Rubin, R., Abbott, L.F., Sompolinsky, H: Balanced excitation and inhibition are required for high-capacity, noise-robust neuronal selectivity. In: *Proceedings of the National Academy of Sciences*, 114(44):E9366–E9375, (2017)
25. Connors, B.W., Long, M.A.: Electrical synapses in the mammalian brain. Ann. Rev. Neurosci. **27**(1), 393–418 (2004)
26. Eugenin, E.A., Basilio, D., Sáez, J.C., Orellana, J.A., Raine, C.S., Bukauskas, F., Bennett, M.V.L., Berman, J.W.: The role of gap junction channels during physiologic and pathologic conditions of the human central nervous system. J. Neuroimmune Pharmacol. **7**(3), 499–518 (2012)
27. Nagy, J.I., Pereda, A.E., Rash, J.E.: Electrical synapses in mammalian cns: past eras, present focus and future directions. Biochim. Biophys. Acta (BBA)-Biomembr. **1860**(1), 102–123 (2018)
28. Sheng, M., Hoogenraad, C.C.: The postsynaptic architecture of excitatory synapses: a more quantitative view. Ann. Rev. Biochem. **76**, 823–847 (2007)
29. Waldvogel, D., van Gelderen, P., Muellbacher, W., Ziemann, U., Immisch, I., Hallett, M.: The relative metabolic demand of inhibition and excitation. Nature **406**(6799), 995–998 (2000)
30. Rash, J.E., Davidson, K.G.V., Kamasawa, N., Yasumura, T., Kamasawa, M., Zhang, C., Michaels, R., Restrepo, D., Ottersen, O.P., Olson, C.O., et al.: Ultrastructural localization of connexins (cx36, cx43, cx45), glutamate receptors and aquaporin-4 in rodent olfactory mucosa, olfactory nerve and olfactory bulb. J. Neurocytol. **34**(3–5), 307–341 (2005)
31. Vivar, C., Traub, R.D., Gutiérrez, R.: Mixed electrical-chemical transmission between hippocampal mossy fibers and pyramidal cells. Eur. J. Neurosci. **35**(1), 76–82 (2012)
32. Hamzei-Sichani, F., Davidson, K.G.V., Yasumura, T., Janssen, W.G.M., Wearne, S.L., Hof, P.R., Traub, R.D., Gutiérrez, R., Ottersen, O.P., Rash, J.E.: Mixed electrical-chemical synapses in adult rat hippocampus are primarily glutamatergic and coupled by connexin-36. Front. Neuroanat. **6**(13), 1–26 (2012)
33. Kuo, S.P., Schwartz, G.W., Rieke, F.: Nonlinear spatiotemporal integration by electrical and chemical synapses in the retina. Neuron **90**(2), 320–332 (2016)
34. Ma, J., Yang, Z.Q., Yang, L.J., Tang, J.: A physical view of computational neurodynamics. J. Zhejiang Univ. Sci. A **20**(9), 639–659 (2019)
35. Beierlein, M., Gibson, J.R., Connors, B.W.: A network of electrically coupled interneurons drives synchronized inhibition in neocortex. Nat. Neurosci. **3**(9), 904–910 (2000)
36. Bucher, D., Prinz, A.A., Marder, E.: Animal-to-animal variability in motor pattern production in adults and during growth. J. Neurosci. **25**(7), 1611–1619 (2005)
37. Marder, E., Bucher, D.: Understanding circuit dynamics using the stomatogastric nervous system of lobsters and crabs. Ann. Rev. Physiol. **69**(1), 291–316 (2007)
38. Nargeot, R., Le Bon-Jego, M., Simmers, J.: Cellular and network mechanisms of operant learning-induced compulsive behavior in aplysia. Curr. Biol. **19**(12), 975–984 (2009)
39. Wenning, A., Norris, B.J., Doloc-Mihu, A., Calabrese, R.L.: Bringing up the rear: new premotor interneurons add regional complexity to a segmentally distributed motor pattern. J. Neurophys. **106**(5), 2201–2215 (2011)
40. Galarreta, M., Hestrin, S.: Electrical synapses between gaba-releasing interneurons. Nat. Rev. Neurosci. **2**(6), 425–433 (2001)
41. Fukuda, T., Kosaka, T.: The dual network of gabaergic interneurons linked by both chemical and electrical synapses: a possible infrastructure of the cerebral cortex. Neurosci. Res. **38**(2), 123–130 (2000)
42. Fukuda, T., Kosaka, T.: Gap junctions linking the dendritic network of gabaergic interneurons in the hippocampus. J. Neurosci. **20**(4), 1519–1528 (2000)

43. Pernelle, G., Nicola, W., Clopath, C.: Gap junction plasticity as a mechanism to regulate network-wide oscillations. PLOS Comput. Biol. **14**(3), 1–29 (2018)
44. Placantonakis, D.G., Bukovsky, A.A., Aicher, S.A., Kiem, H.P., Welsh, J.P.: Continuous electrical oscillations emerge from a coupled network: a study of the inferior olive using lentiviral knockdown of connexin36. J. Neurosci. **26**(19), 5008–5016 (2006)
45. Connors, B.W.: Synchrony and so much more: Diverse roles for electrical synapses in neural circuits. Dev. Neurobiol. **77**(5), 610–624 (2017)
46. Llinas, R., Baker, R., Sotelo, C.: Electrotonic coupling between neurons in cat inferior olive. J. Neurophysiol. **37**(3), 560–571 (1974)
47. Hinrichsen, C.F.L.: Coupling between cells of the trigeminal mesencephalic nucleus. J. Dent. Res. **49**(6), 1369–1373 (1970)
48. Deans, M.R., Volgyi, B., Goodenough, D.A., Bloomfield, S.A., Paul, D.L.: Connexin36 is essential for transmission of rod-mediated visual signals in the mammalian retina. Neuron **36**(4), 703–712 (2002)
49. Pan, F., Paul, D.L., Bloomfield, S.A., Völgyi, B.: Connexin36 is required for gap junctional coupling of most ganglion cell subtypes in the mouse retina. J. Comp. Neurol. **518**(6), 911–927 (2010)
50. Bartos, M., Vida, I., Jonas, P.: Synaptic mechanisms of synchronized gamma oscillations in inhibitory interneuron networks. Nat. Rev. Neurosci. **8**(1), 45–56 (2007)
51. Roxin, A., Brunel, N., Hansel, D.: Role of delays in shaping spatiotemporal dynamics of neuronal activity in large networks. Phys. Rev. Lett. **94**(23), 238103 (2005)
52. Ermentrout, B.: Neural networks as spatio-temporal pattern-forming systems. Rep. Progress Phys. **61**(4), 353–430 (1998)
53. Townsend, R.G., Gong, P.: Detection and analysis of spatiotemporal patterns in brain activity. PLoS Comput. Biol. **14**, 1–29 (2018)
54. Traub, R.D., Jefferys, G.R., Whittington, M.A.: Fast oscillations in cortical circuits. MIT press, Cambridge, MA (1999)
55. Buzsáki, G., Wang, X.-J.: Mechanisms of gamma oscillations. Ann. Rev. Neurosci. **35**, 203–225 (2012)
56. Fisahn, A., Pike, F.G., Buhl, E.H., Paulsen, O.: Cholinergic induction of network oscillations at 40 hz in the hippocampus in vitro. Nature **394**(6689), 186–189 (1998)
57. Buzsáki, G., Chrobak, J.J.: Temporal structure in spatially organized neuronal ensembles: a role for interneuronal networks. Curr. Opin. Neurobiol. **5**(4), 504–510 (1995)
58. Benardo, L.S.: Recruitment of gabaergic inhibition and synchronization of inhibitory interneurons in rat neocortex. J. Neurophysiol. **77**(6), 3134–3144 (1997)
59. Skinner, F.K., Zhang, L., Velazquez, J.L.Perez, Carlen, P.L.: Bursting in inhibitory interneuronal networks: a role for gap-junctional coupling. J. Neurophysiol. **81**(3), 1274–1283 (1999)
60. Söhl, G., Maxeiner, S., Willecke, K.: Expression and functions of neuronal gap junctions. Nat. Rev. Neurosci. **6**(3), 191–200 (2005)
61. Tang, G., Xu, K., Jiang, L.: Synchronization in a chaotic neural network with time delay depending on the spatial distance between neurons. Phys. Rev. E **84**(4), 046207 (2011)
62. Xu, K., Maidana, J.P., Castro, S., Orio, P.: Synchronization transition in neuronal networks composed of chaotic or non-chaotic oscillators. Sci. Rep. **8**(8370), 1–12 (2018)
63. Börgers, C.: An Introduction to Modeling Neuronal Dynamics. Springer, New York (2017)
64. Börgers, C., Kopell, N.: Synchronization in networks of excitatory and inhibitory neurons with sparse, random connectivity. Neural Comput. **15**(3), 509–538 (2003)
65. Rakshit, S., Bera, B.K., Ghosh, D., Sinha, S.: Emergence of synchronization and regularity in firing patterns in time-varying neural hypernetworks. Phys. Rev. E **97**(5), 052304 (2018)
66. Rakshit, S., Bera, B.K., Ghosh, D.: Synchronization in a temporal multiplex neuronal hypernetwork. Phys. Rev. E **98**(3), 032305 (2018)
67. Rakshit, S., Ray, A., Bera, B.K., Ghosh, D.: Synchronization and firing patterns of coupled rulkov neuronal map. Nonlinear Dyn. **94**(2), 785–805 (2018)
68. Rakshit, S., Bera, B.K., Bollt, E.M., Ghosh, D.: Intralayer synchronization in evolving multiplex hypernetworks: analytical approach. SIAM J. Appl. Dyn. Syst. **19**(2), 918–963 (2020)
69. Gray, C.M., König, P., Engel, A.K., Singer, W.: Oscillatory responses in cat visual cortex exhibit inter-columnar synchronization which reflects global stimulus properties. Nature **338**(6213), 334–337 (1989)
70. Uhlhaas, P., Pipa, G., Lima, B., Melloni, L., Neuenschwander, S., Nikolić, D., Singer, W.: Neural synchrony in cortical networks: history, concept and current status. Front. Integr Neurosci. **3**(17), 1–17 (2009)
71. Keane, A., Gong, P.: Propagating waves can explain irregular neural dynamics. J. Neurosci. **35**(4), 1591–1605 (2015)
72. Muller, L., Destexhe, A.: Propagating waves in thalamus, cortex and the thalamocortical system: experiments and models. J. Physiol. Paris **106**(5–6), 222–238 (2012)
73. Mehring, C., Hehl, U., Kubo, M., Diesmann, M., Aertsen, A.: Activity dynamics and propagation of synchronous spiking in locally connected random networks. Biol. Cybern. **88**(5), 395–408 (2003)
74. Yger, P., El Boustani, S., Destexhe, A., Frégnac, Y.: Topologically invariant macroscopic statistics in balanced networks of conductance-based integrate-and-fire neurons. J. Comput. Neurosci. **31**(2), 229–245 (2011)
75. Voges, N., Perrinet, L.U.: Complex dynamics in recurrent cortical networks based on spatially realistic connectivities. Front. Comput. Neurosci. **6**(41), 1–19 (2012)
76. Martens, E.A.: Bistable chimera attractors on a triangular network of oscillator populations. Phys. Rev. E **82**(1), 016216 (2010)
77. Omelchenko, I., Maistrenko, Y., Hövel, P., Schöll, E.: Loss of coherence in dynamical networks: spatial chaos and chimera states. Phys. Rev. Lett. **106**(23), 234102 (2011)
78. Tian, C., Cao, L., Bi, H., Xu, K., Liu, Z.: Chimera states in neuronal networks with time delay and electromagnetic induction. Nonlinear Dyn. **93**(3), 1695–1704 (2018)
79. Martens, E.A., Laing, C.R., Strogatz, S.H.: Solvable model of spiral wave chimeras. Phys. Rev. Lett. **104**(4), 044101 (2010)

80. Bera, B.K., Rakshit, S., Ghosh, D., Kurths, J.: Spike chimera states and firing regularities in neuronal hypernetworks. Chaos Interdiscip. J. Nonlinear Sci. **29**(5), 053115 (2019)
81. Kundu, S., Majhi, S., Ghosh, D.: Chemical synaptic multiplexing enhances rhythmicity in neuronal networks. Nonlinear Dyn. **98**(3), 1659–1668 (2019)
82. Majhi, S., Bera, B.K., Ghosh, D., Perc, M.: Chimera states in neuronal networks: a review. Physi. Life Rev. **28**, 100–121 (2019)
83. Omel'chenko, E., Maistrenko, Y.L., Tass, P.A.: Chimera states: the natural link between coherence and incoherence. Phys. Rev. Lett. **100**(4), 044105 (2008)
84. Tinsley, M.R., Nkomo, S., Showalter, K.: Chimera and phase-cluster states in populations of coupled chemical oscillators. Nat. Phys. **8**(9), 662–665 (2012)
85. Hizanidis, J., Kouvaris, N.E., Zamora-López, G., Díaz-Guilera, A., Antonopoulos, C.G.: Chimera-like states in modular neural networks. Sci. Rep. **6**(1), 1–10 (2016)
86. Majhi, S., Perc, M.: Chimera states in a multilayer network of coupled and uncoupled neurons. Chaos Interdiscip. J. Nonlinear Sci. **22**(7), 073109 (2017)
87. Calim, A., Hövel, P., Ozer, M., Uzuntarla, M.: Chimera states in networks of type-i morris-lecar neurons. Phys. Rev. E **98**(6), 062217 (2018)
88. Wang, X.-J., Buzsáki, G.: Gamma oscillation by synaptic inhibition in a hippocampal interneuronal network model. J. Neurosci. **16**(20), 6402–6413 (1996)
89. Palmigiano, Agostina, Geisel, Theo, Wolf, Fred, Battaglia, Demian: Flexible information routing by transient synchrony. Nat. Neurosci. **20**(7), 1014–1022 (2017)
90. Hodgkin, A.L., Huxley, A.F.: A quantitative description of membrane current and its application to conduction and excitation in nerve. J. Physiol. **117**(4), 500–544 (1952)
91. Koch, C., Segev, I.: Methods in neuronal modeling: from ions to networks. MIT press, Cambridge (1997)
92. Sterratt, D., Graham, B., Gillies, A., Willshaw, D.: Principles of computational modelling in neuroscience. Cambridge University Press, Cambridge (2011)
93. Watts, D.J., Strogatz, S.H.: Collective dynamics of 'small-world' networks. Nature **393**(6684), 440–442 (1998)
94. Golomb, D., Rinzel, J.: Dynamics of globally coupled inhibitory neurons with heterogeneity. Phys. Rev. E **48**(6), 4810 (1993)
95. Golomb, D., Rinzel, J.: Clustering in globally coupled inhibitory neurons. Phys. D Nonlinear Phenom. **72**(3), 259–282 (1994)
96. Kuramoto, Y.: Chemical oscillations, waves, and turbulence. Courier Corporation, Hawaii (2003)
97. Bertolotti, E., Burioni, R., di Volo, M., Vezzani, A.: Synchronization and long-time memory in neural networks with inhibitory hubs and synaptic plasticity. Phys. Rev. E **95**(1), 012308 (2017)
98. Shanahan, M.: Metastable chimera states in community-structured oscillator networks. Chaos Interdiscip. J. Nonlinear Sci. **20**(1), 013108 (2010)
99. Crodelle, J., Zhou, D., Kovačič, G., Cai, D.: A computational investigation of electrotonic coupling between pyramidal cells in the cortex. J. Comput. Neurosci. **48**(4), 387–407 (2020)
100. Baptista, M.S., Kakmeni, F.M.M., Grebogi, C.: Combined effect of chemical and electrical synapses in hindmarsh-rose neural networks on synchronization and the rate of information. Phys. Rev. E **82**(3), 036203 (2010)
101. Liu, C., Wang, J., Yu, H., Deng, B., Wei, X., Tsang, K., Chan, W.: Impact of delays on the synchronization transitions of modular neuronal networks with hybrid synapses. Chaos Interdiscip. J. Nonlinear Sci. **23**(3), 033121 (2013)
102. Sporns, O.: Networks of the Brain. MIT press, Cambridge (2010)
103. Rabinovich, M.I., Huerta, R., Varona, P., Afraimovich, V.S.: Transient cognitive dynamics, metastability, and decision making. PLOS Comput. Biol. **4**(5), 1–9 (2008)